Active High-Power RF Pulse Compression Using Optically Switched Resonant Delay Lines

Sami G. Tantawi, *Member, IEEE,* Ronald D. Ruth, Arnold E. Vlieks, and Max Zolotorev

***Abstract*— We present the design and a proof of principle experimental results of an optically controlled high-power RF pulse-compression system. In principle, the design should handle a few hundreds of megawatts of power at X-band. The system is based on the switched resonant delay-line theory [1]. It employs resonant delay lines as a means of storing RF energy. The coupling to the lines is optimized for maximum energy storage during the charging phase. To discharge the lines, a high-power microwave switch increases the coupling to the lines just before the start of the output pulse. The high-power microwave switch required for this system is realized using optical excitation of an electron–hole plasma layer on the surface of a pure silicon wafer. The switch is designed to operate in the TE_{01} mode in a circular waveguide to avoid the edge effects present at the interface between the silicon wafer and the supporting waveguide; thus, enhancing its power handling capability.**

***Index Terms*—Photoconductive devices, photnic switching systems, pulse compression methods, pulse generation.**

I. Introduction

DURING the past few years, high-power RF pulse-compression systems have developed considerably. These systems provide a method for enhancing the peak power capability of high-power RF sources. One important application is driving accelerator structures. In particular, future linear colliders, such as the proposed next linear collider (NLC) [2], require peak RF powers which cannot be generated by the current state-of-the-art microwave tubes [3].

The SLED pulse-compression system [4] was implemented to enhance the performance of the two-mile accelerator structure at Stanford Linear Accelerator Center (SLAC). One drawback of SLED is that it produces an exponentially decaying pulse. To produce a flat pulse and to improve the efficiency, the binary pulse-compression (BPC) system [5] was invented. The BPC system has the advantage of 100% intrinsic efficiency and a flat output pulse. Also, if one accepts some efficiency degradation, it can be driven by a single power source [6]. However, the implementation of the BPC [7] requires a large assembly of over moded waveguides, making it expensive and extremely large in size. The SLED II pulse-compression system is a variation of SLED which gives a flat output pulse [8]. The SLED II intrinsic efficiency is higher than SLED [9], but not as good as BPC. However, from the compactness point of view, SLED II is far superior to BPC. In this paper, we present a variation on SLED II which will enhance its intrinsic efficiency without increasing its physical size.

The SLED II pulse-compression system employs high Q resonant delay lines to store the energy during most of the duration of the incoming pulse. The round-trip time of an RF signal through one of the delay lines determines the length of the compressed pulse. To discharge the lines, the phase of the incoming pulse is reversed 180° so that the reflected signal from the inputs of the lines and the emitted field from the lines add constructively, thus forming the compressed high-power pulse.

To improve the efficiency of SLED II, we change the coupling coefficient of the storage RF lines during the discharging phase. We designed a fast high-power microwave switch. It is based on bulk effects in semiconductors [10]–[12]. The system is similar to photoconductive switches used in inductive pulsed power systems [12], [13]. We show a design which can handle, in principle, multimegawatt microwave signals. Past experience with high-power microwave ceramic windows [14] suggests that we will have a higher peak-power handling capability by avoiding any electrical field at the interface between the semiconductor wafer and the walls of the supporting waveguide. Hence, we designed the switch to operate at the TE_{01} mode in a circular waveguide.

In Section II, we introduce a theory for optimizing the efficiency of the pulse-compression system using one change in line coupling just before the discharging phase.

In Section III, we analyze a symmetric three-port device. We explore the ability of controlling the coupling between two of the ports by actively changing the termination of the third port. We derive general expressions for power losses and peak electric field in that third arm, which we shall call the active arm. In Section IV, we present the design of the optical switch. In Section V, we describe the implementation of the system and present some experimental results.

II. Active Pulse Compression Using Single-Event Switched Resonant Delay Lines

The theory of active pulse compression with several time events is detailed in [1]. Here, we describe the special case of a *single-event* switched pulse-compression system.

Manuscript received December 5, 1996; revised May 14, 1997. This work was supported by the U.S. Department of Energy under Contract DE-AC03-76F00515.

S. G. Tantawi is with Stanford Linear Accelerator Center (SLAC), Stanford University, Stanford, CA 94309, USA, and with the Electrical Communications and Electronics Department, Cairo University, Giza, Egypt.

R. D. Ruth and A. E. Vlieks are with Stanford Linear Accelerator Center (SLAC), Stanford University, Stanford, CA 94309, USA.

M. Zolotorev is with Lawrence Berkeley Laboratory, Berkeley, CA 94720 USA.

Publisher Item Identifier S 0018-9480(97)06018-3.

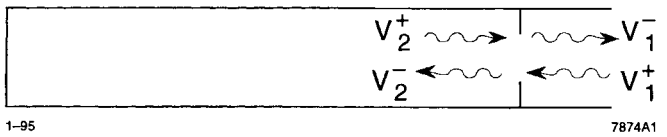

Fig. 1. Resonant delay line.

A. Passive Pulse Compression

Consider the waveguide delay line with a coupling iris shown in Fig. 1. The *lossless* scattering matrix representing the iris is unitary. At a certain reference plane the matrix takes the following form:

$$\underline{\underline{S}} = \begin{pmatrix} -R_0 & -j\left(1-R_0^2\right)^{1/2} \\ -j\left(1-R_0^2\right)^{1/2} & -R_0 \end{pmatrix}. \tag{1}$$

With the exception of some phase change, the incoming signal V_2^+ at time instant t is the same as the outgoing signal V_2^- at time instant $t-\tau$, where τ is obviously the round-trip delay through the line; i.e., $V_2^+(t) = V_2^-(t-\tau)e^{-j2/\beta}$, where β is the wave propagation constant within the delay line, and l is the length of the line. During the charging phase, we assume a constant input, i.e., $V_1^+(t) = V_{\text{in}}$ which equals a constant value. We also assume that all the voltages are equal to zero at time $t < 0$. Furthermore, if the delay line has small losses (β has a small imaginary part), at resonance the term $e^{-j2\beta l} = -p$, where p is a positive real number close to 1. Hence,

$$V_1^-(i) = -V_{\text{in}}\left[R_0 - \left(1-R_0^2\right)\frac{1-(R_0p)^i}{1-R_0p}p\right]. \tag{2}$$

In (2), $V_1^-(i)$ means the outgoing wave in the time interval $i\tau \le t < (i+1)\tau$ and $i \ge 0$. After the energy has been stored in the line one may dump part of the energy in a time interval τ by flipping the phase of the incoming signal just after a time interval $(n-1)\tau$, i.e.,

$$V_1^+(t) = \begin{cases} V_{\text{in}}, & 0 \le t < (n-1)\tau \\ -V_{\text{in}}, & (n-1)\tau \le t < n\tau \\ 0, & \text{otherwise.} \end{cases} \tag{3}$$

The output pulse level during the time interval $(n-1)\tau \le t < n\tau$ is then

$$V_{\text{out}} = V_1^-(n-1) = V_{\text{in}}\left[R_0 + \left(1-R_0^2\right)\frac{1-(R_0p)^{n-1}}{1-R_0p}p\right]. \tag{4}$$

Indeed, this is the essence of the SLED II pulse-compression system.

The maximum power gain of SLED II is limited. The power gain as $n \to \infty$ has a maximum value of

$$\text{Maximum Power Gain} = \frac{17}{p^2} - 8 - \frac{12\sqrt{2(1-p^2)}}{p^2} \tag{5}$$

which occurs at

$$R_0 = \frac{1}{p} - \frac{\sqrt{8(1-p^2)}}{4p}.$$

Clearly, the maximum power gain is limited to 9 as $p \to 1$. Furthermore, this maximum is greatly affected by the losses in the delay line. For example, the gain is limited to 7.46 if the line has a 1% round-trip power losses.

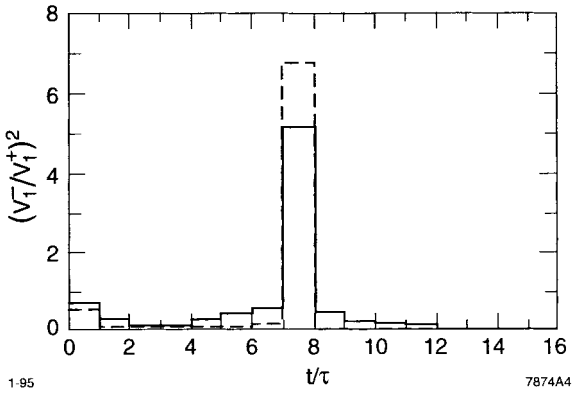

Fig. 2. Comparison between SLED II output and a one-time switched resonant delay line for a compression ration of 8. The line is switched just before the last time bin. The thick curve represents switched line, and the thin curve represents SLED II.

B. Active Switching During Delay-Line Discharge

To discharge the line, one can keep the input signal at a constant level during the time interval $0 \le t < n\tau$, but switching the iris reflection coefficient to zero so that all the energy stored in the line is dumped out. However, to reduce the burden on the switch, one can reverse the phase together with changing the iris reflection coefficient. In this case, all the energy can still be dumped out of the line, but the iris reflection coefficient need not be reduced completely to zero. During the discharge interval the new iris S-matrix parameters can be written in the following form:

$$\underline{\underline{S}} = \begin{pmatrix} -\cos(\theta) & -j\sin(\theta) \\ -j\sin(\theta) & -\cos(\theta) \end{pmatrix}. \tag{6}$$

During the last time bin we set $V_2^- = 0$, which leads us to write

$$R_d = \cos\left[\tan^{-1}\left(\frac{1-(R_0p)^{n-1}}{1-R_0p}\left(1-R_0^2\right)^{1/2}p\right)\right]. \tag{7}$$

This new reflection coefficient is greater than zero and the switch need only change the iris between R_0 and R_d. The output then reduces to

$$V_{\text{out}} = R_d\left[1 + \left(\frac{1-(R_0p)^{n-1}}{1-R_0p}\right)^2\left(1-R_0^2\right)p^2\right]V_{\text{in}}. \tag{8}$$

The compressed pulse takes place in the interval $(n-1)\tau \le t < n\tau$. The optimum value of R_0 is such that it fills the system with maximum possible amount of energy in the time interval $(n-1)\tau$. Fig. 2 shows both the optimum pulse shapes of SLED II and SLED II with active discharge switch.

For the case of discharging by active switching, the maximum power is

$$\text{Maximum Power Gain} = \frac{p^2}{1-p^2} \tag{9}$$

which occurs at $R_0 = p$. Unlike the passive system, the maximum power gain has no intrinsic limit. It is only limited

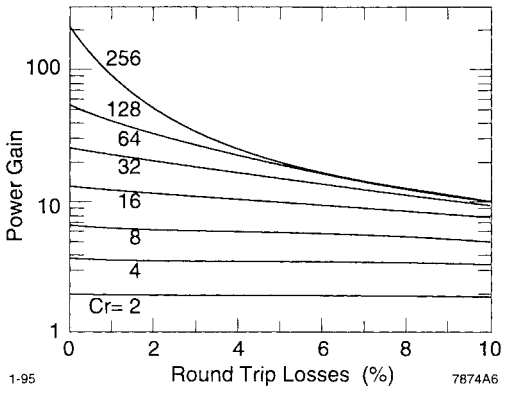

Fig. 3. Effect of line and switching iris losses on compression efficiency for a one-time switched resonant delay line.

by the amount of losses in the storage line. In this case, the gain can be much higher than nine, which is the limit of the passive system.

C. Effect of Losses

As the compression ratio increases, the stored energy spends more time in the storage lines resulting in a reduction in efficiency due to the finite quality factor of the lines. Fig. 3 shows the effect of losses for different compression ratios. The round-trip line loss plus reflection losses at the end of the line plus reflection losses at the active iris is defined as

$$\text{Round Trip Powers Loss} = 1 - p^2.$$

D. Comparison

Table I compares the two types of pulse-compression systems. It also gives the optimum system parameters for each compression ratio C_r; here C_r is defined as the total time interval divided by the duration of the compressed pulse, i.e., n. The efficiency of the system η is defined as the energy in the compressed pulse divided by the total incident energy, namely, $\eta = \frac{1}{C_r}\left(\frac{V_{\text{out}}}{V_{\text{in}}}\right)^2$. In these calculations we assume a lossless system, i.e., $p = 1$.

In general, switching the line just before the last time bin is the most advantageous technique. For reasonably high compression ratios the change in the iris reflection coefficient is relatively small. This simplifies the high-power implementation of the active iris. The losses in the delay line also make the efficiency of the system deteriorates with higher compression ratios. Clearly, the active system is advantageous at high compression ratios. However, it soon loses its advantage because of delay-line losses. Between the compression ratios of 6 and 32, the active system has a significant advantage over the passive one. At the same time, the delay-line losses do not reduce its efficiency in a significant way.

TABLE I
COMPARISON BETWEEN DIFFERENT METHODS OF SINGLE-EVENT SWITCHING PULSE-COMPRESSION SYSTEMS

C_r	SLED II		Discharging Just Before The Last Time Bin		
	η (%)	Opt. R_0	η (%)	Opt. R_0	R_d
2	78.1	0.5	100	0.0	0.707
4	86.0	0.607	87.0	0.646	0.536
6	74.6	0.685	84.9	0.775	0.443
8	64.4	0.733	84.0	0.835	0.386
12	49.9	0.792	83.1	0.892	0.317
16	40.6	0.828	82.7	0.920	0.275
32	23.3	0.893	82.0	0.960	0.195
64	12.6	0.936	81.7	0.980	0.138
128	6.6	0.962	81.6	0.990	0.099
256	3.4	0.978	81.5	0.995	0.069

III. MICROWAVE CONTROL USING A SYMMETRIC THREE-PORT NETWORK

Consider a passive microwave network which is composed of a basic *lossless* three-port device with two similar ports—namely, ports 1 and 2. The third port is terminated so that all the scattered power from that port is completely reflected. However, the phase of the reflected signal from the third port can be changed actively. For any lossless and reciprocal three-port network, the scattering matrix is unitary and symmetric. By imposing these two conditions on the scattering matrix $\underline{\underline{S}}$ of our device and at the same time taking into account the symmetry between port 1 and port 2, at some reference planes, one can write

$$\underline{\underline{S}} = \begin{pmatrix} \frac{e^{j\phi}-\cos\theta}{2} & \frac{-e^{j\phi}-\cos\theta}{2} & \frac{\sin\theta}{\sqrt{2}} \\ \frac{-e^{j\phi}-\cos\theta}{2} & \frac{e^{j\phi}-\cos\theta}{2} & \frac{\sin\theta}{\sqrt{2}} \\ \frac{\sin\theta}{\sqrt{2}} & \frac{\sin\theta}{\sqrt{2}} & \cos\theta \end{pmatrix}. \tag{10}$$

Indeed, with the proper choice of the reference planes, this expression is quite general for any symmetric three-port network. The scattering matrix properties are determined completely with only two parameters: θ and ϕ. The scattered RF signals $\underline{V}^-$ are related to the incident RF signals $\underline{V}^+$ by

$$\underline{V}^- = \underline{\underline{S}}\,\underline{V}^+ \tag{11}$$

where $V_i^{\pm}$ represents the incident/reflected RF signal from the ith port. We terminate the third port so that all the scattered power from that port is completely reflected, i.e.,

$$V_3^+ = V_3^- e^{j\psi}. \tag{12}$$

The resultant symmetric two-port network then has the following scattering matrix parameters:

$$S_{11} = S_{22} = \frac{(e^{j\psi} + e^{j\phi}) - (1 + e^{j(\phi+\psi)})\cos\theta}{2(1 - \cos\theta e^{j\psi})} \tag{13}$$

$$S_{12} = S_{21} = \frac{(e^{j\psi} - e^{j\phi}) - (1 - e^{j(\phi+\psi)})\cos\theta}{2(1 - \cos\theta e^{j\psi})}. \tag{14}$$

By changing the angle ψ of the third-port terminator, the coupling between the first and the second ports can vary from 0 to 1.

The signal level at the third arm is then given by

$$|V_3^+|^2 = |V_3^-|^2 = \frac{\sin^2\theta}{3 - 4\cos\theta\cos\psi + \cos 2\theta}|V_1^+ + V_2^+|^2. \tag{15}$$

This signal level is independent of the parameter ϕ and has a maximum or a minimum value at $\psi = 0$ or π.

IV. The Optical Switch

A. Device Physics

To actively change the angle of the reflection coefficient at the third port we place a piece of semiconductor material in the third arm. An external stimulus such as a laser light can induce an electron–hole plasma layer at the surface of the semiconductor, thus changing its dielectric constant. Therefore, the propagation constant of RF signals through the active arm changes, and consequently, the coupling between the other two ports also changes.

For the pulse-compression system application associated with the NLC [2], for which we choose a compression ratio of eight, it is required to change the reflection coefficient at the first arm between two fixed values. The device should remain in one state for approximately 1.75 μs, and in the other state for 250 ns. Since silicon has a carrier lifetime which can extend from 1 μs to 1 ms, it seems like a natural choice for this application. One can excite the plasma layer with a very short pulse from the external stimulus ($\sim$ 5 ns) and the device will stay in its new status longer than the duration of the RF signal. Since repetition rate for this pulse-compression system is 180 pulse/s there is sufficient time between pulses for the switch to completely recover.

To be useful, this switch needs to have a very small amount of losses. By comparing estimates of the collision frequency for silicon [15] to 11.424 GHz, the operating frequency of the NLC, one can readily show that the dielectric constant of a the semiconductor material is given by the classical relation

$$\varepsilon = \varepsilon_0\varepsilon_r\left(1 - j\frac{\sigma}{\omega\varepsilon_0\varepsilon_r}\right) \tag{16}$$

where

$$\sigma = e\sum_i \mu_i N_i \tag{17}$$

which is the conductivity of the semiconductor. In the above equations, ω is the radial frequency of the RF signal, m_i^* is the effective mass of carrier i (electron, light hole, and heavy hole), N_i is carrier density, e is the electron charge, and v_i is the collision frequency.

To minimize the losses in the off state, i.e., when there is no plasma excited, we need to have a very pure semiconductor material such that the intrinsic carrier density is very small. In the *on* state, i.e., when the plasma layer is excited, the carrier density should be large enough so that the semiconductor acts like a good conductor, thus minimizing the losses.

At a carrier density of 10^{19}/cm^3, silicon has a conductivity of $\sim 3.3 \times 10^2$ mho/cm. This is three orders of magnitude smaller than that of copper. However, it is high enough to make an effective reflector. The skin depth of an RF signal at the NLC frequency at this conductivity level is ~ 8 μm. In choosing the laser wavelength to produce the photo-induced carriers, light penetration depth should be comparable to this skin depth.

B. Design Methodology

While charging the delay line with RF energy, the reflection coefficient of the coupling iris is R_0, as given in Table I for different compression ratios. Hence, we choose the angle ψ_c, which is the angle of the reflection coefficient of the third arm during the charging time, so that $|S_{11}|^2 = R_0^2$. During the charging time, we choose the angle $\psi_c = \pi$. Equation (13) then becomes

$$R_0^2 = \sin^2\frac{\phi}{2} \tag{18}$$

which determines the angle ϕ completely. During the charging time, the charging signal is constant and is equal to V_{in}. Hence, using (15) and theory presented in Section II, one can write an expression for the field level in the control arm (the third arm) as follows:

$$\begin{aligned}|V_3^+| &= |V_3^-| \\ &= \frac{1}{\sqrt{2}}\tan\frac{\theta}{2}\left|j\frac{1-(R_0p)^{C_r-2}}{1-R_0p}\left(1-R_0^2\right)^{1/2}p+1\right|V_{\text{in}}.\end{aligned} \tag{19}$$

During the discharging time, the angle ψ would change from π to the new value ψ_d, Hence, the active layer, i.e., a silicon wafer will be placed at a point which has a reduced electric field by a factor of $\sin\psi_d$. One then writes an expression for the maximum field seen by the silicon wafer during the charging time as follows:

$$\begin{aligned}E_{\max} = 2&\left|\tan\frac{\theta}{2}\cos\frac{\psi_d}{2}\right|\left|j\frac{1-(R_0p)^{C_r-2}}{1-R_0p}\left(1-R_0^2\right)^{1/2}p+1\right| \\ &\times\left(\frac{P_{\text{in}}Z_3}{A_3G_3}\right)^{1/2}\end{aligned} \tag{20}$$

where P_{in} is the constant level input power, Z_3 is the wave impedance of the mode excited in the waveguide which forms the third arm, A_3 is the cross-sectional area of that guide, and G_3 is the geometrical factor which depends on the mode and the waveguide shape of the third arm. The angle ψ_d should satisfy

$$\begin{aligned}|S_{11}|^2 &= R_d^2 \\ &= \frac{\left(\cos\left(\frac{\phi+\psi_d}{2}-\theta\right)+\cos\left(\frac{\phi+\psi_d}{2}+\theta\right)-2\cos\left(\frac{\phi-\psi_d}{2}\right)\right)^2}{4-8\cos(\psi_d)\cos(\theta)+4\cos^2(\theta)}\end{aligned} \tag{21}$$

where R_d is given by (7), and its numerical values is tabulated in Table I. Finally, at the discharging time we evaluate the signal level at the third arm which leads us to write an

expression for the amount of losses in the silicon wafer during the discharging time, P_l as follows:

$$P_l = \left(\frac{2\sin\theta}{(3 - 4\cos\theta\cos\psi_d + \cos 2\theta)^{1/2}} \times \left| j\frac{1-(R_0 p)^{C_r - 1}}{1 - R_0 p}(1 - R_0^2)^{1/2} p - 1 \right| \right)^2 \frac{R_s}{Z_3} P_{\text{in}} \tag{22}$$

where R_s is the surface resistance and is given by $R_s = (\frac{\omega\mu_0}{2\sigma})^{1/2}$. The value of the conductivity σ is given by (17). One clearly wants to use as much laser power as possible to maximize σ.

Equations (18), (20)–(22) are the design equations. The goal of the design is to reduce the electric field below 100 kV/cm during the charging time, which is the estimated breakdown field for a silicon wafer with a relatively large size. We assume that we can achieve this value although experimental data on photoconductive switches showed lower values [16] for the breakdown field because we will not be using any metallization on the edges of the silicon wafer. We will also try to use an electromagnetic mode which does not have any normal electric fields near the edges of the silicon wafer. At the same time, one should keep the losses in the silicon wafer below a certain limit so that the temperature of the wafer does not rise above a certain temperature—say, 70 °C. If this temperature is exceeded, a risk of thermal runaway exists. As the silicon wafer gets hotter, the losses during discharging time increase, causing the temperature to rise further until the silicon wafer becomes conductive because of thermal effects alone.

C. Switching Time

The calculations of the switching time of this system is governed by the filling time of the third arm. To calculate this time accurately one must know how all the system components behave with frequency. This is beyond the scope of the current analysis. However, one can have a conservative estimate for that time by considering only the third arm at resonance. If this arm has an approximate length of one-half wavelength, and couples to the outside world with an iris which has a reflection coefficient equal to $\cos\theta$ [$S_{33} = \cos\theta$; see (10)] the filling time T_f can then readily be shown to be

$$T_f = \frac{-\left(1 - \left(\frac{f_c}{f}\right)\right)^{-1/2}}{f\ln(\cos\theta)} \tag{23}$$

where f is the operating frequency. This equation assumes that the third port is at resonance; however, in the real operation of the switch the third arm is never brought to resonance. Hence, the expression puts an upper limit on the switching time.

D. Design Example

The power required to be generated from an RF station in the NLC test accelerator [2] is 400 MW at a pulsewidth of 250 nS, at 11.424 GHz. This can be produced using the proposed 75-MW klystrons [17] while compressing the output of these klystrons with a compression ratio of 8 and assuming a compression efficiency of 75%. To compress the RF signal efficiently by a factor of eight, the magnitude of the reflection coefficient of an iris needs to change between 0.835–0.386. We choose to operate the active arm at the TE_{01} mode of a circular waveguide. We choose this mode of operation because it has no normal field near the walls. Hence, one need not worry about the details of high field operation at the interface between the silicon wafer and the waveguide walls [14], [18]. The geometrical factor G_3, which appears in (20) equals 0.479 for that mode. Then, using (18), the angle $\phi = 113.23°$. We choose the radius of the third arm to be 2.78 cm. This radius will allow the TE_{01} mode to propagate and will cutoff the TE_{02} mode. We then choose the angle $\theta = 122.4°$. This will make the rise time of the switch less than 2 nS (23). To satisfy (21), the angle $\psi_d = 202.97°$. The field amplitude in the third arm during the charging time is estimated with the help of (20) to be 95.5 kV/cm. Finally, according to (22), the losses of the switch during the discharging time is 4.5%.

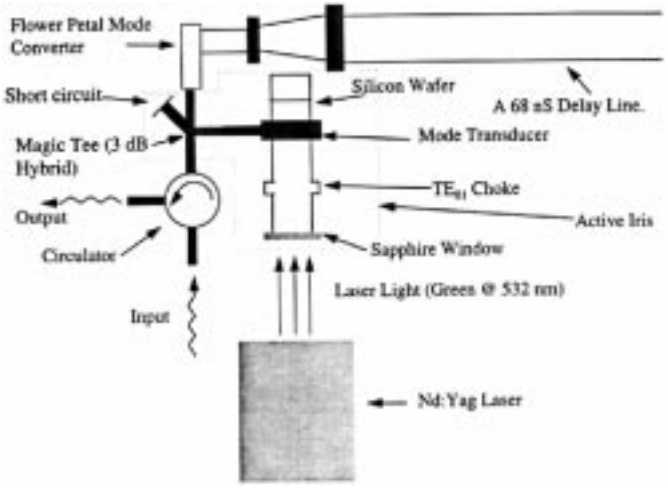

Fig. 4. Schematic diagram of the proof-of-principle experiment.

V. Proof-of-Principle Experiment

Fig. 4 shows the schematic diagram of an active pulse-compression experiment. A flower-petal mode transducer [19] and a long circular waveguide act as the storage delay line. The waveguide is excited at the TE_{01} mode. A matched magic tee (3-dB hybrid), terminated with a short circuit at the E-arm acts as the three-port network. The TE_{01} mode switching arm (third arm) is connected to the H-arm of the magic tee with a special side-coupled mode converter [20]. The circular guide, representing the third arm, is terminated from one side by a short circuit plate and a 250-μm-thick, 6000-Ω cm silicon wafer is placed between the shorting plate and the mode converter. From the other side of the mode converter, a TE_{01} choke acts as a terminator for this circular guide while allowing the laser light to reach the silicon wafer.

The movable short, which is connected to the E-arm of the magic tee, is tuned until the reflection coefficient reaches R_0. Then, the laser is fired and the silicon wafer position is adjusted to get a reflection coefficient equals to R_d.

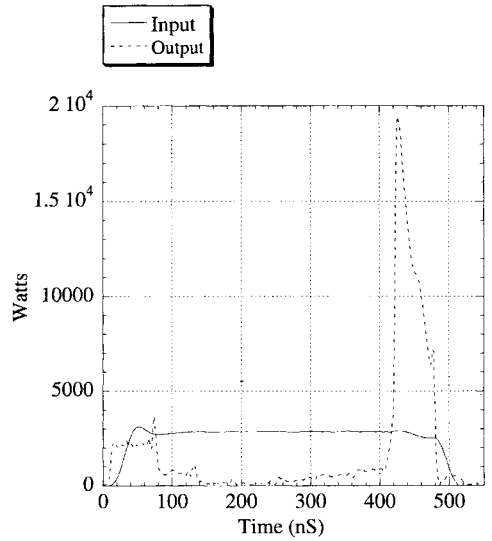

Fig. 5. Experimental output of the active pulse-compression system at a compression ratio of eight.

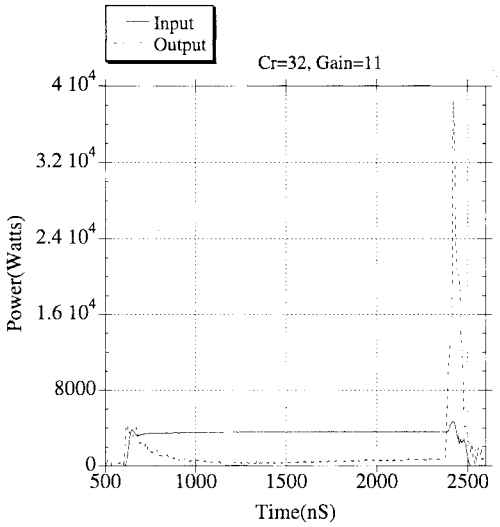

Fig. 6. Experimental output of the active pulse-compression system at a compression ratio of 32.

Fig. 5 shows the output of this system at a compression ratio of eight. The system has a gain of six. The passive pulse-compression system, SLED II, has a theoretical gain of 5.1, and if one assumes similar losses in the delay-line, SLED II gain would drop to 4.2. Fig. 6 shows the output of the system for a compression ratio of 32. The system has a gain of 11. SLED II has a theoretical gain of 7.4, and if one assume similar losses in the delay-line, SLED II gain would drop to ~ 5. Indeed, a gain of 11 is much more than the theoretical gain of any passive pulse-compression system. These have a maximum gain of nine as the compression ratio goes to infinity.

VI. Conclusion

We have developed the theory for a single-time-switched resonant delay-line pulse-compression system. We gave a design example for an active iris operating at the TE_{01} mode. Finally, we demonstrated the operation of such a switch. The system achieved a power gain of 11 at a compression ratio of 32. This is more than the maximum theoretical gain of SLED II even as the compression ratio goes to infinity.

Acknowledgment

The authors wish to thank Prof. K. Zaki, Electrical Engineering Department, University of Maryland at College Park, for suggesting to the first author, S. G. Tatawi, that devices based on bulk effect in semiconductors could be useful even at power levels as high as a few tens of megawatts. The authors also thank Prof. W. Vernon, University of California at San Diego, for suggesting that bulk effects in semiconductors could develop a useful technique for RF pulse compression. The authors also appreciate the help of T. G. Lee, especially during the mechanical design phase of this device.

References

[1] S. G. Tantawi *et al.*, "Active RF pulse compression using switched resonant delay lines," *Nuc. Instrum. Methods Phys. Res. A, Accel. Spectrom. Detect. Assoc. Equip.*, vol. 370, pp. 297–302, 1996.

[2] R. D. Ruth *et al.*, "The next linear collider test accelerator," in *Proc. IEEE Particle Accelerator Conf.*, Washington DC, May 1993, pp. 543–545.

[3] *Proc. Conf. Pulsed RF Sources for Linear Colliders*, Montauk, Long Island, NY, Oct. 2–7, 1994.

[4] Z. D. Farkas *et al.*, "SLED: A method of doubling SLAC's energy," in *Proc. 9th Int Conf. High Energy Accelerators*, Stanford, CA, May 1974, pp. 576–579.

[5] Z. D. Farkas, "Binary peak power multiplier and its application to linear accelerator design," *IEEE Trans. Microwave Theory Tech.*, vol. MTT–34, pp. 1036–1043, Oct. 1986.

[6] P. E. Latham, "The use of a single source to drive a binary peak power multiplier," in *Linear Accelerator Conf.*, Williamsburg, VA, Oct. 1988, pp. 623–624.

[7] Z. D. Farkas *et al.*, "Two-klystron binary pulse compression at SLAC," in *Proc. IEEE Particle Accelerator Conf.*, Washington DC, May 1993, pp. 1208–1210.

[8] P. B. Wilson, Z. D. Farkas, and R. D. Ruth, "SLED II: A new method of RF pulse compression," presented at the *Linear Accl. Conf.*, Albuquerque, NM, Sept. 1990.

[9] Z. D. Farkas *et al.*, "Radio frequency pulse compression experiments at SLAC," presented at the *SPIE's Symp. High Power Lasers*, Los Angeles, CA, Jan. 1991.

[10] C. H. Lee, Ed., *Picosecond Optoelectronic Devices*. New York: Academic, 1984.

[11] C. H. Lee, "Optical control of semiconductor closing and opening switches," *IEEE Trans. Electron Devices*, vol. 37, pp. 2426–2438, Dec. 1990.

[12] A. Rosen and R. Zutavern, Eds., *High-Power Optically Activated Solid-State Switches*. Norwood, MA: Artech House, 1994.

[13] E. E. Funk *et al.*, "80-kW inductive pulsed power system with a photoconductive semiconductor switch," *IEEE Photon. Technol. Lett.*, vol. 3, pp. 576–577, June 1991.

[14] W. R. Fowkes *et al.*, "Reduced field TE_{01} X-band traveling wave window," presented at the *Proc. 16th IEEE Particle Accelerator Conf. (PAC'95) and Int. Conf. High-Energy Accelerators (IUPAP)*, Dallas, Texas, May 1–5, 1995.

[15] S. M. SZE, *Physics of Semiconductor Devices*. New York: Wiley, 1969.

[16] G. M. Loubriel *et al.*, "Photoconductive semiconductor switches for pulsed power applications," in *Proc. 9th IEEE Pulsed Power Conf.*, Albuquerque, NM, June 1993, pp. 76–79.

[17] D. Sprehn *et al.*, "PPM focused X-band klystron development at the Stanford linear accelerator center," in *Proc. 3rd Int. Workshop RF Pulsed Power Sources for Linear Colliders (RF'96)*, Hayama, Japan, Apr. 8–12, 1996.

[18] S. G. Tantawi *et al.*, "Design of a multi-megawatt X-band solid state microwave switch," presented at the *IEEE Int. Conf. Plasma Sci.*, Madison, WI, June 1995.

[19] S. G. Tantawi *et al*., "Numerical design and analysis of a compact TE_{01} to TE_{11} mode transducer," in *Conf. Computational Accelerator Physics*, Los Alamos, NM, Feb. 1993, pp. 99–106.
[20] S. G. Tantawi *et al*., "Compact TE_{10} (rectangular) to TE_{01} (circular) mode converter for over moded waveguides," U.S. Patent S-85 926 (RL-13545) Apr. 30, 1996.

Sami G. Tantawi (S'88–M'88) was born in Giza, Egypt, in 1962. He received the B.Sc. and M.Sc. degrees in electrical engineering from Cairo University, Giza, Egypt, in 1984, and 1987, respectively, and the Ph.D. degree in electrical engineering from the University of Maryland at College Park, in 1992.

He has been a Staff Physicist with the Stanford Linear Accelerator Center (SLAC), Stanford, CA, since 1992, where he is responsible for designing and implementing high-power RF pulse-compression systems. He is also with the Electrical Communications and Electronics Department, Cairo University, Giza, Egypt. His research interests include vacuum electronics, high-power RF devices, modeling of RF structures, and planner RF circuits.

Ronald D. Ruth received the B.A. degree in mathematics and physics from the University of Iowa, Iowa City, in 1973, the M.A. and the Ph.D. degrees, both in physics, from the State University of New York at Stony Brook (SUNY), in 1978 and 1981, respectively.

From 1974 to 1977, he was an Instructor in the Department of Physics, Southern Connecticut State College. From 1981 to 1984, he was a Staff Scientist at Lawrence Berkeley Laboratory. From 1982 to 1983, he was a Scientific Associate at CERN. From 1984–1991, he was a Staff Physicist at Stanford Linear Acceleration Center (SLAC), Stanford, CA. In 1991, he was an Associate Professor at SLAC, and is currently a Professor there. His research interests included accelerator and particle beam physics, nonlinear effects, collective instabilities in storage rings and linacs, high-gradient linear acceleration, next-generation linear colliders.

Dr. Ruth is a Fellow of the American Physical Society since 1984.

Arnold E. Vlieks received the B.S. degree in physics from Rensselaer Polytechnic Institute, Troy, NY, in 1966, and the M.S. and Ph.D. degrees in physics from Ohio State University, Columbus, in 1971 and 1973, respectively.

From 1973 to 1976 he was a Post-Doctoral Fellow and Lecturer at the University of Toronto. From 1976 to 1978, he was a Visiting Foreign Researcher at CNRS, Orsay, France. From 1978 to 1980, he was a Post-Doctoral Fellow at the University of Zuerich, Switzerland. From 1980 to 1982, he was a Post-Doctoral Fellow at the University of Muenster, Germany. From 1982 to 1985, he was with the Litton Electron Device Division, Litton Industries. Since 1985, he has been with the Stanford Linear Accelerator Center (SLAC), Stanford University, Stanford, CA. He became Group Leader of the Klystron R&D Group where he worked on such programs as the high-power relativistic klystron program in a collaboration with LLNL and the X-band klystron for SLAC's Next Linear Collider (NLC) program. Since 1992, he has been Group Leader of the NLC R&D Structures Group. His work deals with the development of low-loss RF components for the NLC, development of a viable pulse-compression system (SLED-II), and the testing of high gradient accelerator structures and components for the NLC.

Max Zolotorev, photograph and biography not available at the time of publication.